Po-production in lead: Calculation and measurement on SINQ-samples (PSI)

Daniela Kiselev[1], Tobias Lorenz[1], Yong Dai[1], Jean-Christophe David[2], Dorothea Schumann[1], Michael Wohlmuther[1]
[1]Paul Scherrer Institut, Switzerland
[2]CEA-Saclay, France

Abstract

The Paul Scherrer Institut operates a MW-class spallation source, SINQ, using the 590 MeV proton beam delivered by the ring cyclotron, HIPA. The target of the spallation source consists of a bundle of lead filled metal tubes (Cannelloni). Five lead samples were extracted from a rod in the target centre close to the beam entrance window from SINQ target-4, which had been in operation since 2000/2001 and received a total integrated beam charge of about 10 Ah. The lead was radiochemically investigated and the activities of several isotopes could be measured. Special attention was paid to Po as it has [illegible]emitting isotopes with considerable half-lives and the element can show – depending on the experimental conditions - distinct volatility properties. A much larger amount of the Po isotopes ^{208}Po (2.9 y), ^{209}Po (102 y) and ^{210}Po (138 d) was found in the samples compared to the prediction obtained with available cross-section models in the particle transport code MCNPX. In particular, the amount of ^{210}Po measured more than 10 years after the target operation is by far too large to be explained by direct production from Bi impurities in the lead. This implies another reaction mechanism not considered in the standard INC (Intranuclear Cascade) and evaporation models. Therefore, a recently improved INC and evaporation model, the Liège intranuclear-cascade model (named INCL) coupled to the de-excitation model ABLA07 was implemented into MCNPX2.7.0. INCL4.6/ABLA07 is one of the most accurate models to describe spallation reactions as an inter-comparison done under the auspices of IAEA demonstrated. In this contribution, preliminary results of the nuclide inventory calculated with MCNPX using INCL4.6/ABLA07 and Bertini-Dresner are presented and compared to the experimental data.

Introduction and motivation

The Paul Scherrer Institut (PSI) operates the High Intensity Proton Accelerator (HIPA), which delivers a continuous proton beam with energy of 590 MeV and a current of up to 2.4 mA. The protons are produced in a compact electron cyclotron resonance (ECR) source [1], which is located in the Crockcroft-Walton. The 870 keV protons are subsequently accelerated in two cyclotrons called injector2 and ring. In the first step, injector2 accelerates the protons to 72 MeV. From there they are injected to the ring cyclotron and finally extracted with an energy of 590 MeV. On their way to the spallation source SINQ, they pass two graphite targets Target M and Target E used for meson production. The latter one has a thickness of 40 mm, which leads to a reduction of the beam energy to 575 MeV as well as beam loss. Due to multiple scattering at Target E, an extended collimator system follows to shape the beam. Including the beam loss at Target E, the beam intensity drops by 30%. In normal operation, the beam is guided to SINQ, where it is fully stopped. The purpose of SINQ is to deliver a high flux of thermal and cold neutrons for e.g. material research. The neutrons are produced in lead, which is packed into about 350 tubes called cannelloni. Today, the cladding consists of zircaloy. Zircaloy absorbs fewer neutrons than steel, which was used formerly. The cannellonis are cooled by D_2O and surrounded by a safety shroud from AlMg3. To date, SINQ is the most powerful continuous spallation neutron source in the world.

Figure 1. Sketch of the lower part of SINQ target-4 with the safety hull, (left) sketch of the beam profile on the first row of cannellonis (right)

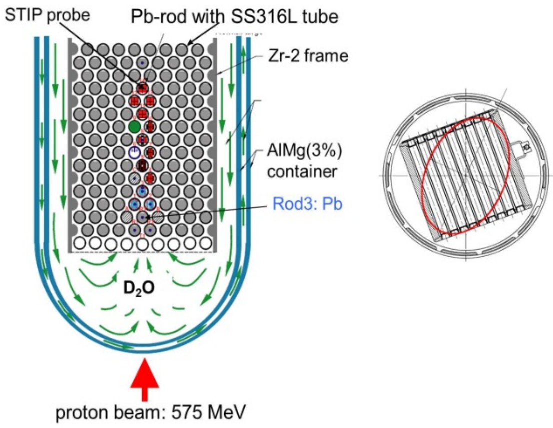

Each SINQ target is irradiated for 2 years. After that it has to be replaced to avoid failure due to radiation damage. The target is highly activated with dose rates around 10 Sv/h after 1 year cooling time in the SINQ target storage. Therefore, it has to be disposed as radioactive waste. The STIP(SINQ Target Irradiation Programme – a research programme aimed to study material properties after high-power proton und neutron exposure) samples, which often contain other materials than lead, are used for post-irradiation examination. They are removed by remote-handling via manipulators in the service cell ATEC. For disposal, the SINQ target is put into a steel container, which is filled with lead-bismuth eutecticum (LBE) for safety reasons. Before the SINQ target can be disposed as radioactive waste, the authorities require – in addition to other documentation – the complete nuclide inventory with radioactive isotopes of half-lifes larger than 60 days. The complete nuclide inventory can only be provided by calculations. For the evaluation of nuclide inventories of directly irradiated components the particle transport Monte Carlo programme MCNPX [2] is used at PSI. The calculated nuclide inventories have to be at least partially validated by comparison with experimental data, i.e. specific activities of relevant isotopes. Particularly interesting are isotopes with are highly radiation hazardous like α-emitters and volatile elements. Some of these isotopes have to be extracted first by radiochemical methods before their activities can be measured. Isotopes with high energetic photons, which are particularly damaging to the human body, are of interest as well. Since MCNPX is also used for other purposes at PSI, it is important to have an estimate of the reliability and uncertainty of its predictions.

Figure 2. Double Gaussian beam distribution from MCNPX, (left) proton flux distribution along Rod3 (right)

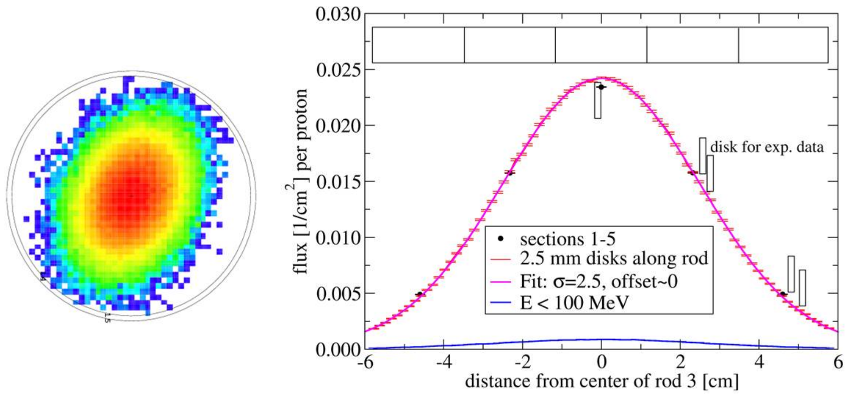

The locations of the sample disks and the partitioning of the rod as used in MCNPX are also shown.

For this purpose, a cannelloni filled with lead was removed from the centre of the second filled row of SINQ target-4. This cannelloni is called Rod3 (see Figure 1). Next to Rod3, left and right as well as downstream, STIP samples were located (see Figure 1). Rod3 was also equipped with a thermocouple, which indicated an operation temperature of 550 +/-30 K, close to but lower than the melting temperature of lead of 600.6 K. Target-4 was in operation in 2000 and 2001, where it received 10.03 Ah protons. The cannellonis of target-4 were still made of stainless steel 316L. The target holder itself had a quadratic cross-section of about 14 cm x 14 cm and was about 40 cm long. The shape of the proton beam on the target window had in good approximation a double Gaussian profile. Since Rod3 is from the centre of the target, the flux distribution of the protons and secondary particles is symmetric along the rod with respect to its centre (see Figure 2). Because Rod3 is located in the second row, the protons are mainly high-energetic and resemble the Gaussian profile of the beam. As expected, the neutron flux distribution is wider than the proton distribution and does not vanish close to the end caps of the rod. For further examination with radiochemical methods, the lead bar of Rod3 was cut into a few disks, each 1.5 mm thick, which later were subdivided. The specific activities of 17 isotopes were measured in five disks. The locations of the disks relative to the centre of Rod3 are indicated in the plot of the proton flux distribution in Figure 2. The activities of the γ-emitters ^{60}Co, ^{101}Rh, ^{102m}Rh, ^{125}Sb, ^{133}Ba, ^{172}Hf, ^{172}Lu, ^{194}Hg, ^{207}Bi were detected by a High Purity Germanium detector (HPGe) [3]. The α-emitters ^{146}Sm, ^{148}Gd, ^{150}Gd, ^{208}Po, ^{209}Po, ^{210}Po had first to be chemically separated and then were measured by an α-analyst spectroscopic system from Canberra using the GENIE-2000 software [4]. The amount of very long-lived isotopes ^{36}Cl and ^{129}I had to be measured by Accelerator Mass spectrometry (AMS) at the ETHZ Hönggerberg after chemical separation for a suitable ion source. The distribution of the specific activities along the rod follows the proton flux distribution for all isotopes – except for two, ^{36}Cl and ^{125}Sb. This suggests another or additional reaction mechanism in addition to the spallation by protons. When the activity of ^{210}Po was determined 10.5 y after end of beam (EOB), it was surprisingly high – much higher than predicted by the available calculations at the time. With a half-life of only 138 d simple back-scaling of activities to EOB would result in an enormous activity of 1.2 10^{13}Bq/g. The measurement was repeated after 1 additional year. The activity of ^{210}Po was almost as high as 1 year ago in the first measurement. This discrepancy triggered the following work.

In this report it will be shown how the nuclide inventory is obtained using MCNPX coupled to build-up and decay codes in general. The post-analysis, necessary before comparing to the experimental results, will be shortly explained. Reaction mechanisms leading to the production of Po-isotopes will be discussed and supported by extracted production cross-sections. As the physics cross-section models implemented in MCNPX2.7.0 could not explain the high activity of ^{210}Po, a new physics model, INCL4.6/ABLA07, was implemented in MCNPX2.7.0. The most important features of INCL4.6/ABLA07, particularly the improvements compared to the older version INCL4.2/ABLA, which is still a model choice in MCNPX2.7.0, will be listed. Finally, the calculated activities using the default model in MCNPX2.7.0 as well as INCL4.6/ABLA07 will be compared to experimental data.

Nuclide inventory by MCNPX

MCNPX can transport all kind of particles, protons, neutrons, pions up to heavy nuclei. Nuclear reactions of these particles have to be handled by physics models, when no cross-section tables are available. Physics models are necessary, since there is no exact theory for the strong interaction yet. Most physics models use, for the SINQ energy range, the microscopic picture of an intranuclear cascade (INC) followed by evaporation or fission. In the first step, the INC, the energy transferred by the primary particle is dissipated in the nucleus to several nucleons by nucleon-nucleon collisions. The INC proceeds until the dissipated energy falls below a specified value, related to the depth of the nuclear potential well, or a stopping time has been reached. The typical duration of the intranuclear cascade is 10^{-22} seconds. During the INC, high energetic particles might be emitted in forward direction by direct reactions, i.e. high-energy transfer from the primary particles to a constituent of the nucleus. If the INC is not able to give a thermalised remnant nucleus, it is followed by a preequilibrium phase. When the INC (with or without a preequilibrium step) is finished, the nucleus is left in an excited state with defined excitation energy and an angular momentum. The number of protons and neutrons residing in the nucleus is usually already less than in the target nucleus, as some particles might have been already emitted. When the excitation energy is high enough, low energetic particles, often neutrons but also light ions and photons, are emitted isotropically at low kinetic energy. This is called evaporation and leads to the reduction of the excitation energy until no particle can be emitted anymore. Depending on the conditions and on the remaining nucleus, fission is a competitive reaction channel.

The INC model BERTINI [5,6] has for years been the default choice in MCNPX for neutrons and protons of energy less than 3.5 GeV. The BERTINI model, which uses a pre-equilibrium step by default, is coupled to the evaporation code of Dresner [7]. The DRESNER code is based on Weisskopf´s statistical model. Fission, if possible, is handled by the RAL code [8]. Since BERTINI can handle only protons and neutrons, reactions containing light ions up to 1 GeV are handed over to ISABEL [9].

In addition to BERTINI and ISABEL, MCNPX2.7.0 contains the Cascade Exciton Model CEM3.03 [10] and INCL4.2/ABLAV3p. CEM is able to emit light ions and clusters up to ^{28}Mg. INCL4.2 has several known shortcomings. For instance, the model cannot form clusters in the cascade state and reaction cross-sections below 100 MeV are severely underestimated. In addition, the version ABLAV3p [11], could only emit neutrons, protons and ^{4}He. Tritons are missing, which means that the tritium content is always underestimated using ABLAV3p. Therefore, INCL was upgraded to INCL4.6 [13] and ABLA to ABLA07 [14]. The new INCL4.6 treats neutrons, protons, pions, deuterons, tritons, ^{3}He and α-particles, i.e. reaction cross-sections are provided for reactions with these particles as projectiles. At the same time, INCL4.6 is also able to emit such particles as well as light fragments up to a mass number of 8 during the intranuclear cascade phase. This is done by forming these clusters by coalescence in phase space. ABLA07 itself is able to generate neutrons, protons, deuterons, tritons, ^{3}He, α-particles as well as intermediate mass fragments (IMF) by break-up, fission or evaporation. A drawback of the new physics model INCL4.6/ABLA07 is that no information of the production of metastable nuclei in the residual state is available. The fraction, which is devoted to the metastable partner, is needed not only for the calculation of metastable nuclei but also for the ground state. This fraction is subtracted from the number of ground state nuclei and therefore reduces its activity. To take this into account, the fractions of metastables produced were taken from the MCNPX default choice. Previously, comparison with measured radioisotope activities provided good results with it, also for metastables like ^{108m}Ag.

In the following work, a comparison of the activities obtained with the MCNPX default physics model and INCL4.6/ABLA07 as well as with data has been made. Since INCL4.6/ABLA07 is not available in one of the officially released versions of MCNPX or MCNP, it was implemented in MCNPX2.7.0 as a replacement for INCL4.2/ABLA. The implementation was performed in such a way that the code runs on several CPU´s in parallel. The final version will be sent to RSICC as a patch (MW) to comply with the regulations for the use of the MCNPX source code. In our upgraded version of MCNPX2.7.0, the production rates obtained from the physics models are not written to the histp-file but appended to the MCNPX output file. Otherwise the histp-file would become dramatically large, which finally would limit the number of primary particles in the simulation. This method is similar to a previous patch for MCNPX2.5.0 included in the CINDER1.05 package from the NEA Data Bank [15]. This package contains also the so-called activation script [16], which simplifies the coupling of the output of MCNPX and decay- and build-up codes to proceed finally to the activities. The decay- and build-up code CINDER1.05 [17] was used in this report and was checked using FISPACT-2007 [18] with EAF-2007 [19].

For neutrons of E<20 MeV, the physics models are not evoked but rather tabulated cross-sections ENDF/B-VI are applied. Therefore, their production rates are not written to file instead the neutron flux up to 20 MeV in each cell is recorded. The neutron flux is later folded by production cross-sections provided by CINDER1.05 or EAF-2007.

The geometrical model used for the calculations in MCNPX is shown in Figure 3. The geometry of the full SINQ monolith, which is available as MCNPX input, was limited to the necessary parts to speed up the Monte Carlo simulation. This is the target with some D_2O (in turquoise) around and part of the steel dump to account for backscattered neutrons. All STIP probes with their different material compositions were modelled as they have a significant influence e.g. on the neutron flux in the SINQ target. The presence of all STIP probes reduces the neutron flux by ca. 20%. To further reduce the computation time to reach sufficient statistics, Rod3 was divided into 5 parts only, one central to the beam. Each part is 2.32 cm long. With disks of 1.5 mm thickness, as they were used in the radiochemical examination, the required statistics could not be reached on a reasonable timescale. The subdivision into five cells, which are much larger than the disks, means that the nuclide inventory calculated is an average over the region of the cell. Moreover, the positions of the experimentally investigated disks do not coincide with the centres of the cells, as shown in Figure 2. In addition, the calculated nuclide inventory was corrected by a factor obtained from the ratio of the proton flux in the disk and in the corresponding cell. This procedure is justified as the radioactive isotopes under consideration are produced mainly by protons – except for the Po isotopes. It turned out that tritons and alphas follow closely the spatial flux distribution of protons along the rod. As expected, tritons and alphas are produced by high energetic protons.

For the results presented in this work, the high performance cluster ROSA in Lugano, Switzerland, was used for the calculations with INCL4.6/ABLA07. To calculate the activities 86016 CPU*h, it was only necessary to count the runs. The total number of primary particles was 3.3 10^9. Other runs like the calculation of the particle fluxes or using pure Pb, are not included in this line-up. These additional simulations amount in about the same order of CPU*h as given above. As MCNPX with the default choice of INC and evaporation models runs much faster, the calculations could be performed on the smaller parallel cluster MERLIN available at PSI. 2.4 10^9 primary particles were collected from different runs in 4704 CPU*h.

Figure 3. Full (reduced) geometrical model used in MCNPX, (left) zoom into the target area (right)

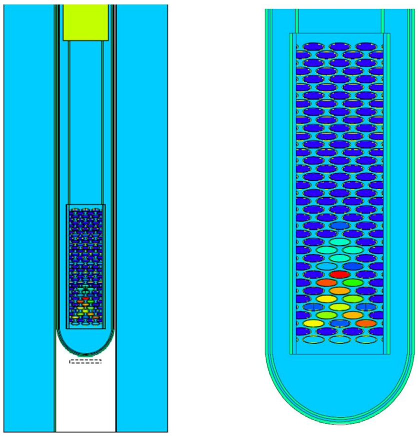

Po-isotopes: Production mechanisms and comparisons of the activities

Using the MCNPX default choice as described above the three relevant Po-isotopes, ^{208}Po, ^{209}Po, ^{210}Po are almost exclusively produced from the Bi impurity in the lead. Since these production mechanisms were known at the design state of SINQ, lead with a low Bi impurity is used. Still, the abundance of Bi in the SINQ lead is 220 ppm [20]. Since Bi has only one stable isotope, ^{209}Bi, the relevant production channels are as follows

^{209}Bi(p,2n)^{208}Po

^{209}Bi(p,n)^{209}Po

^{209}Bi(p,γ)^{210}Po, ^{209}Bi(n,γ)^{210}Bi $\rightarrow$ ^{210}Po

For the ^{210}Po production clearly the n-capture is the dominant reaction mechanism and leads to a large activity of the order of MBq/g ^{210}Po in the lead of the SINQ target after end of operation. ^{210}Bi decays with a half-life of 5 min into ^{210}Po. According to the MCNPX default physics model no other reaction mechanism leads to a significant contribution. Since ^{210}Po has a half-life of 138 d, the ^{210}Po activity should be well below 1 Bq/g after 10 years cooling time. This prediction is in strong disagreement with the recent measurement performed at PSI [4]. Therefore, other reaction mechanisms were considered. The double n-capture on ^{208}Pb is negligible, particularly since ^{209}Pb has a half-life of 3 h and the neutron fluxes in the SINQ target are moderate. Nevertheless, the reaction channel is considered in the Cinder1.05 library. A promising reaction mechanism is ^{208}Pb(t,p)^{210}Pb, where ^{210}Pb decays with a half-life of 22 years to ^{210}Bi, which almost instantaneously decays into ^{210}Po. As described above INCL4.6 is able to simulate reactions with tritons as well as to produce tritons as secondary particles from the proton nuclear reaction, which is a prerequisite. The triton energy spectrum as well as its cross-sections on ^{208}Pb to ^{210}Pb was explicitly calculated with INCL4.6 and MCNPX default settings. The comparison is shown in Figure 4. The tail to higher energies of the triton spectrum obtained by INCL4.6 is striking compared to MCNPX default. This is surely a consequence of the new feature in INCL4.6 to emit high energetic tritons during the INC phase. In spite of this, the peak at about 20 MeV is a bit higher. The low energetic tritons are mostly produced by evaporation, i.e. ABLA07. A more dramatic difference is seen in the triton production cross-section for ^{210}Pb. On the linear scale, the result from MCNPX2.7.0 default cannot be seen as it is 4 orders of magnitude lower. The cross-section from INCL4.6 is of the order of 20 mbarn at its maximum, at 25 MeV. It is concentrated in a small band of +/- 5 MeV around the maximum. Therefore, the high energetic tritons do not contribute much to the production cross-section of ^{210}Pb. A triton energy distribution as obtained by MCNPX default using the INCL4.6 cross-section would lead to about a factor 2 to 3 lower production rate only.

Figure 4. Triton flux obtained with the two physics models in MCNPX

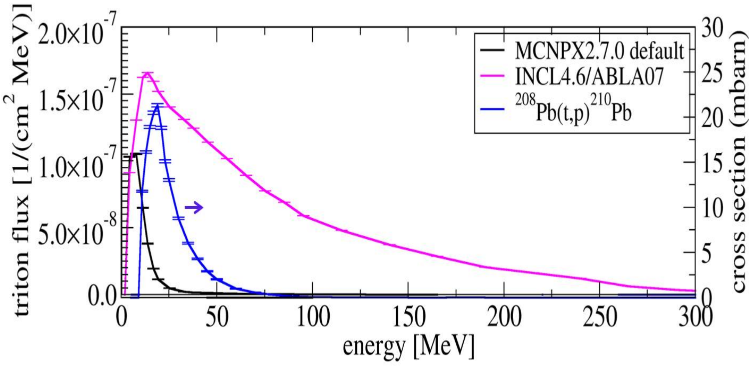

Blue curve: Cross-section for the reaction $^{208}Pb(p,t)^{210}Pb$ (right axis).

The time dependence of the ^{210}Po specific activity is shown in Figure 5 for the central part of Rod3. It illustrates and confirms the considerations above. Using MCNPX default the ^{210}Po activity simply decays with its half-life of 138 d. 7-8 years after end of operation the decay curve slows down. After 9 years the activity is completely determined by the decay of ^{210}Pb, which is produced in very small quantities by MCNPX with default settings. However, the measured ^{210}Po activity after 10.5 years is about 5 orders of magnitude larger than obtained with MCNPX default. The new implemented physics model INCL4.6/ABLA07 leads to a production of ^{210}Pb in a much larger amount. It was obtained by folding the calculated triton spectrum with the corresponding production cross-section depicted in Figure 4. However, the statistics for the reaction channel was still unsatisfactory. Nevertheless, the ^{210}Pb production rate calculated with MCNPX plus INCL4.6/ABLA07 agreed within a factor of less than 2 in all 5 cells of Rod3 with the one obtained by folding. Already after 3 years the activity of ^{210}Po is in radioactive balance with ^{210}Pb, which is about 5 orders of magnitude larger than calculated with MCNPX default.

Figure 5. Predicted time dependence of ^{210}Po after end of beam (EOB) using the two physics models and comparison to the experimental data point

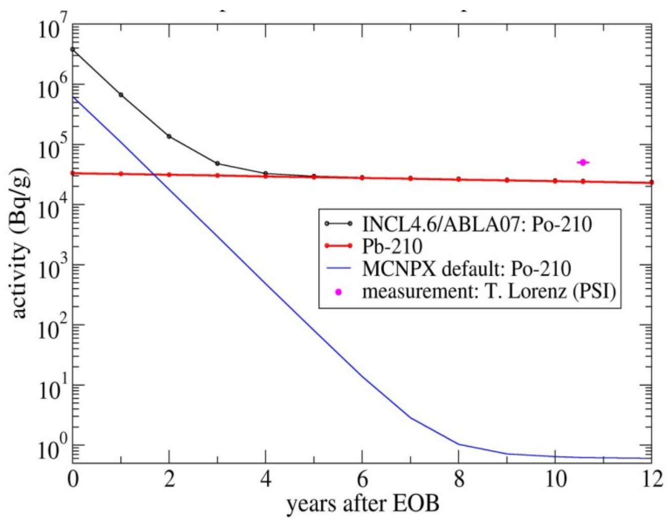

Figure 6. Ratio of simulated and measured activities, averaged over the different measured locations, 10.5 y after EOB

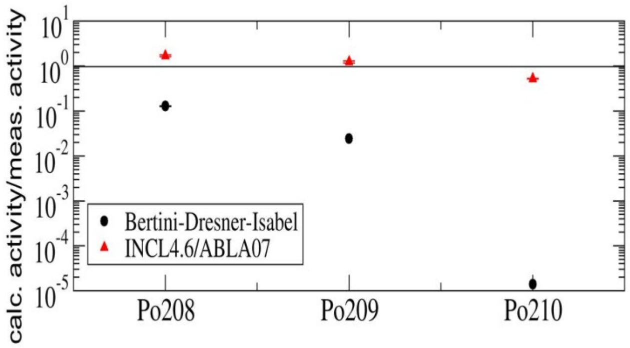

The specific activities of ^{210}Po, ^{208}Po and ^{209}Po, obtained with INCL4.6/ABLA07, are remarkable close to the experimental data points (see Figure 6). The comparison to the data is made at the measurement date, about 10.5 years after end of operation. The results depicted in Figure 6 were averaged over the different measurement locations. The time dependent behaviour of ^{208}Po and ^{209}Po was also checked. It corresponded to a pure decay, i.e. no other isotopes are contributing to it.

It should be noted that the ^{210}Po activity just after end of operation is about 5 times larger using INCL4.6/ABLA07 compared with MCNPX default (see Figure 5 at 0 years). This contribution cannot result from the Bi impurity, since the same tabulated neutron cross-sections were used in MCNPX applying the two physics models, which leads to the same neutron flux spectra below 20 MeV. A test run with pure Pb confirmed this assumption. In addition, the production of ^{208}Po and ^{209}Po is also increased by a factor of 10 and 100, respectively. This is clearly seen in Figure 6, when compared with the results from MCNPX default. This means that the Bi impurity is not the main source of the Po production anymore. It contributes about 20% to the ^{210}Po activity in the first years before ^{210}Po is produced via ^{210}Pb. Bi only contributes only 10% and 1% to the production of ^{208}Po and ^{209}Po, respectively. The reaction channels, which produce the Po isotopes from the stable Pb isotopes are driven by alphas this time. In Figure 7, the ^{208}Po production cross-section is shown for alpha particles on three Pb isotopes ^{206}Pb, ^{207}Pb, ^{208}Pb. The cross-sections obtained by INCL4.6/ABLA07 are 4 to 5 orders of magnitude larger than extracted from MCNPX default simulations. Two sets of experimental data [21-22] are in very good agreement with the predictions of INCL4.6/ABLA07. If one compares the cross-sections from ISABEL for the three Pb isotopes relative to each other, they show at least the same order as the ones from INCL4.6/ABLA07.

Figure 7. ^{208}Po production cross-section by alpha reaction on Pb isotopes

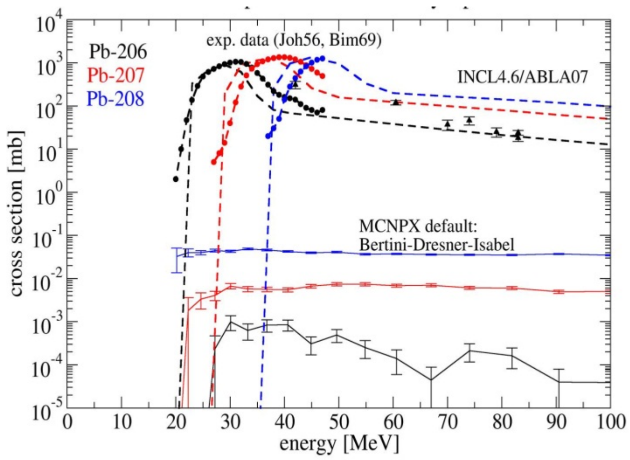

Figure 8 shows the spatial distribution of the calculated Po activities along the rod using INCL4.6/ABLA07 in logarithm scale and the spatial distribution is compared to the data. The error bars of the calculation are purely statistical. They result from the statistical error of the production rate calculations. As expected from the reaction mechanisms and keeping in mind that the spatial flux distribution of tritons and alphas are very similar, the calculated spatial distributions of the activities of the three Po isotopes are very similar and follow the proton flux distribution. The comparison to the experimental data is satisfactory and is a significant improvement compared to MCNPX default.

Figure 8. Spatial distribution of the three Po isotopes along Rod3

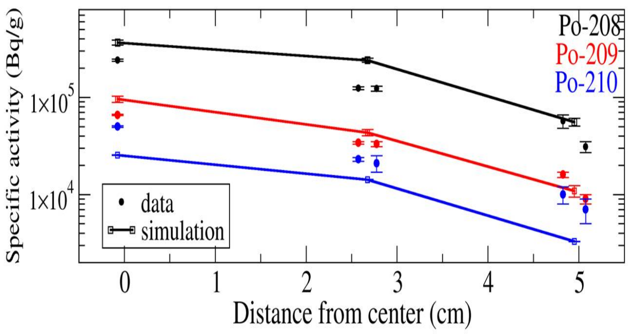

Comparison of the results obtained with INCL4.6/ABLA07 and measurement.

Comparison of the calculated and measured activities for the remaining isotopes

In addition to Po, the activities of 12 γ-emitters and two long-lived isotopes were measured at different positions along Rod3. The isotopes were already listed above. Since it is not feasible to show all comparisons in detail in this report, first a comparison of the spatial distributions along Rod3 for the activities obtained with INCL4.6/ABLA07 and MCNPX default was made. This would allow observing large differences and might suggest different production mechanisms. As can be seen in Figure 9, the variation of the ratio of the activities calculated with INCL4.6/ABLA07 and MCNPX default is between 0.2 and 2.5. In most of the cases, MCNPX default predicts larger activities. For most of the isotopes, the distribution of the activities is the same, i.e. the ratio is roughly constant. The largest difference appears for ^{36}Cl and ^{148}Gd. Far from the centre of Rod3, INCL4.6/ABLA07 predicts almost a factor two larger activity of ^{36}Cl. As this isotope showed a broader spatial distribution in the measurement, it will be investigated in more detail below.

Figure 9. Ratio of activities obtained by MCNPX using INCL4.6/ABLA07 and BERTINI-DRESNER-ISABEL

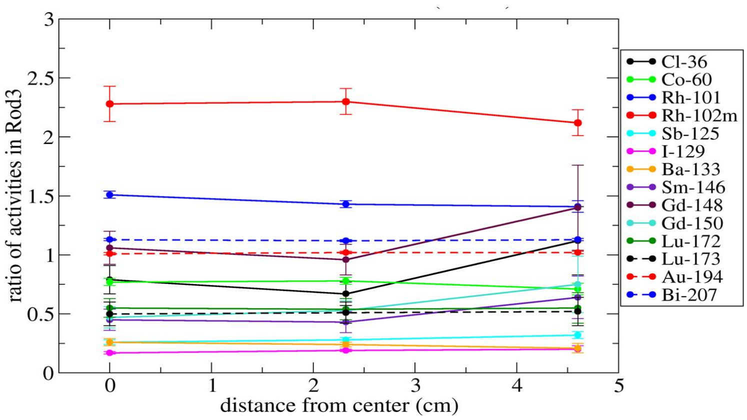

Figure 10. Comparison of the calculation using the two physics models to the measured activities of the remaining isotopes

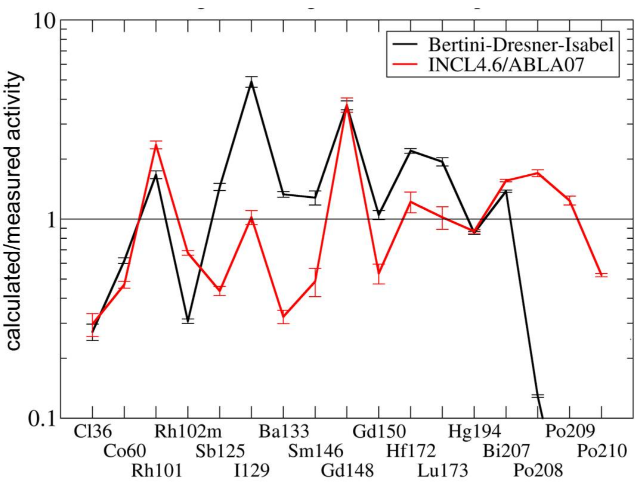

A comparison with the experimental data is shown for both physics models in Figure 10. The ratio of the calculated to measured activities is the weighted average over the results obtained at the measured locations. The experimental data, which are spatially close to each other, were averaged first. Excluding the Po-isotopes in the following discussion, the deviation of the calculated activity to the measured one is less than a factor of four for both physics models. The largest deviations appear for ^{36}Cl and ^{102m}Rh. The prediction for ^{102m}Rh could be improved by INCL4.6/ABLA07 by a factor 2. A significant improvement can also be noted for ^{129}I. On the other hand, ^{133}Ba is worse predicted than in MCNPX default. Altogether both physics models show a similar behaviour and agreement.

In Figure 11, a detailed comparison for ^{36}Cl activity is presented as a function of the position in Rod3. The experimental data seems to be quite independent of the position. There is some spread of the data and the uncertainties are larger compared to other isotopes. This is due to the difficult preparation and measurement via AMS. As already mentioned, both physics models predict similar ^{36}Cl activities. At the centre of Rod3, they both match well with the measurement. The disagreement becomes obvious when compared with the data at the tail of Rod3. In the simulation, ^{36}Cl is produced by spallation only, mainly from Pb, as the elemental composition of Pb used in MCNPX contains no Cl. Therefore the spatial distribution of the calculated activity follows the proton flux distribution. INCL4.6/ABLA07 slightly deviates from this at the outer region of Rod3. However, the reason why Cl is not in the material composition of Pb, is that it could not be measured in [20]. The method used is ICP-OES, i.e. inductively coupled plasma optical emission spectroscopy. Via n-capture on Cl ^{36}Cl is produced. Therefore elemental Cl would certainly broaden the spatial distribution of the activity along Rod3, since the neutron flux distribution is much broader and particularly has much more strength at the tail of the rods. Therefore some Cl was added to the material composition defined in MCNPX using INCL4.6/ABLA07 and its effect studied. It turned out that a tiny fraction of 0.5 ppm Cl is enough to match quite well the measured activities (see Figure 11). It seems that even less (about a factor 2) might be sufficient to explain the trend of the data.

Figure 11. Spatial distribution of the ^{36}Cl activity comparing calculations and measurement

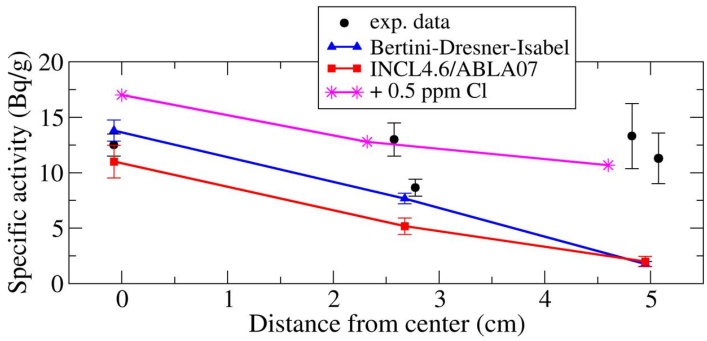

Figure 12. Spatial distribution of the ^{125}Sb activity comparing calculations and measurement

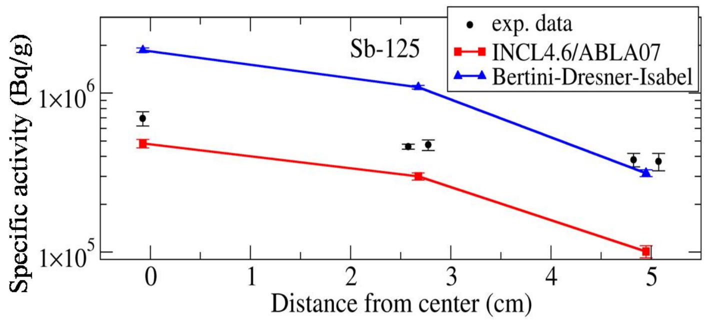

A similar trend of the data is observed for ^{125}Sb. The results are shown at the date of measurement in November 2011 in Figure 12. The results from both physics models follow the shape of the proton distribution. The difference between them is a factor 3 whereas the experimental data are somehow in between the two predictions. Similar to the case of ^{36}Cl, we looked deeper into possible reaction mechanisms with a neutron involved as the primary particle to broaden-up the spatial distribution. Two ideas came up. Neutron capture on ^{124}Sn leads to ^{125}Sn, which decays with a half-life of 2.8 y to ^{125}Sb. This process is driven by low-energy neutrons and is included in the Cinder1.05 library. The abundance of Sn in the material definition of Pb is 100 ppm. However, the isotope fraction for ^{124}Sn is only 5%. A second possibility would be double neutron capture on ^{123}Sb. The interim state has a half-life of only 60 d, which reduces the probability of a second neutron capture. In order to determine the contribution to the ^{125}Sb production for both reaction mechanisms, both elements, Sn and Sb, were removed from the Pb composition. It turned out that their contribution to ^{125}Sb production is negligible. Since the reaction mechanisms described above strongly depend on the corresponding cross-sections in the build-up and decay code, the analysis was performed also with FISPACT-2007 using EAF-2007. There were no additional contributions to the production of ^{125}Sb in agreement with CINDER1.05. The discrepancy between the measured data and the calculation is not solved yet.

Summary and outlook

Knowledge of the nuclide inventory of highly activated components is important to make provisions during operation in case of an accident as well as for the later disposal as radioactive waste. The nuclide inventory is provided by calculations and therefore needs to be validated by measurements. In the spallation target-4 of SINQ at PSI, the activities of 17 isotopes were measured at positions in the lead material of one cannelloni, which is located central and close to the proton beam entrance window. Ten years after the end of operation of the target, a 5 orders of magnitude, a larger activity was measured for ^{210}Po compared with predictions from the calculations available at this time (MCNPX with default physics model). In addition, ^{210}Po decayed much slower than expected. This led to the conclusion that ^{210}Po is fed by ^{210}Pb, which can be produced by tritium reaction on ^{208}Pb. As the cross-section for this reaction is negligible for the default physics model in MCNPX, BERTINI-DRESNER-ISABEL, a new intranuclear cascade model INCL4.6 plus the evaporation/fission code ABLA07 was implemented in MCNPX2.7.0 in a way to allow for parallel computation and to avoid huge data output (histp-file). Good agreement with the measured ^{210}Po activity as well as the ^{208}Po and ^{209}Po activities was found using INCL4.6/ABLA07. The spatial distribution along the rod is well reproduced, too. The ^{208}Po and ^{209}Po, ^{210}Po activities were also a factor 10, 100 and 5 higher than predicted with MCNPX default. Reactions with alphas on the lead isotopes leading to ^{208}Po, ^{209}Po, ^{210}Po were not accounted for properly in the previous calculation. This means that all Po-isotopes are mainly produced from lead and not from the Bi impurity as predicted by MCNPX default choice.

For the remaining isotopes, differences between BERTINI-DRESNER-ISABEL and INCL4.6/ABLA07 are less than a factor 5. The largest deviation from the data is observed for ^{36}Cl. The measured activities of ^{36}Cl and ^{125}Sb show along the rod a much flatter distribution than the calculations, which follow the shape of the proton beam. This suggests reactions with low energetic neutrons which are more evenly distributed due to isotropic evaporation from the nuclei. The material definition used for the calculation does not contain Cl, because it could not be detected with ICP-OES. The addition of 0.5 ppm Cl considerably improved the agreement with the data. Although ^{125}Sb can also be produced by neutrons from ^{124}Sn or ^{123}Sb, the contribution is small according to the calculation. No reaction mechanism was found to explain the flat distribution of the measured activity for ^{125}Sb.

As interest in comparing the measured Po data with other codes was great during the workshop, a benchmark will be organised involving all state-of-the-art codes FLUKA [23], GEANT[24], MARS [25] and PHITS [26] in addition to MCNPX2.7.0. PHITS already uses INCL4.6/ABLA07 by default and A. Ferrari has a private version of FLUKA with INCL4.6/ABLA07 for testing [27]. The benchmark will be performed first on a simplified toy model, a lead block surrounded by D_2O, to avoid large running times (still the computer power needed is considerable) and the additional time to code the detailed geometry. A comparison with MCNPX using INCL4.6/ABLA07 will be made with other physics models available in MCNPX2.7.0. In particular, ISABEL will be used as INC model not invoking BERTINI to check, if the coupling between BERTINI and ISABEL has an influence on the treatment of reactions with tritons and alphas. Y. Yariv is working on an improved version, ISABEL2. For this, a comparison of the cross-sections for the relevant reaction channels will be made.

On the experimental side, there is on-going work to measure the spatial distribution of the activities of several isotopes in three more rods from the same SINQ target-4. One rod will be in the fourth filled row not in a central position, the other one is roughly in the centre of the target in a central position. The last rod is located in the last row and in the outermost position. Therefore, additional interesting data for comparisons will become available.

Acknowledgements

This work was supported by a grant from the Swiss National Supercomputing Centre (CSCS) under project PSI. Part of the calculations was performed at the HPC Merlin4 cluster at PSI.

References

[1] C. Baumgarten, A. Barchetti, H. Einenkel, D. Goetz, P.A. Schmelzbach (2011), “A compact electron cyclotron resonance proton source for the Paul Scherrer Institute's proton accelerator facility”, *Rev. Sci. Instrum.*, 82[5], 053304.

[2] D.B. Pelowitz (2011), “MCNPX user’s manual – version 2.7.0”, LA-CP-11-00438.

[3] T. Lorenz, Y. Dai, D. Schumann (2013), “Analysis of long-lived radionuclides produced by proton irradiation in lead targets –γ- Measurements”, *Radiochim. Acta*, 101[10], pp. 661-666.

[4] T. Lorenz, Y. Dai, D. Schumann, A. Türler (2014),“Proton-induced Polonium Production in Lead”, *Nucl. Data Sheets*.

[5] H.W. Bertini (1963), “Low-Energy Intranuclear Cascade Calculation”, *Phys. Rev.,* 131, pp. 1801-1821.

[6] H.W. Bertini (1969), “Intranuclear-Cascade Calculation of the Secondary Nucleon Spectra from Nucleon-Nucleus Interactions in the Energy Range 340 to 2900 MeV and Comparisons with Experiment”, *Phys. Rev.,* 188, pp. 1711-1730.

[7] L. Dresner(1981), “EVAP-A Fortran Program for Calculating the Evaporation of Various Particles from Excited Compound Nuclei”, *Oak Ridge National Laboratory report ORNL-TM-7882*.

[8] F. Atchison (2007), “A treatment of medium-energy particle induced fission for spallation-systems’ calculations”, *Nucl. Instr. Meth.* B, 259, pp. 909-932.

[9] Y.Yariv, Z.Fraenkel (1979), “Intranuclear cascade calculation of high-energy heavy-ion interactions”, *Phys. Rev. C*, 20, pp. 2227-2243; dito (1981),“Intranuclear cascade calculation of high energy heavy ion collisions: Effect of interactions between cascade particles”, *Phys. Rev. C*, 24,pp. 488-494.

[10] S.G. Mashnik, A.J. Sierk (2012), “CEM3.03 User Manual”, *LANL Report LAUR-12-01364*, Los Alamos, US.

[11] J.-J. Gaimard, K.-H. Schmidt (1991), “A reexamination of the abrasion-ablation model for the description of the nuclear fragmentation reaction”, *Nucl. Phys. A*, 531, pp. 709-745.

[12] A.R. Junghans, M. de Jong, H.-G. Clerc, A.V. Ignatyuk, G.A. Kudyaev, K.-H. Schmidt (1998), "Projectile-fragment yields as a probe for the collective enhancement in the nuclear level density", *Nucl. Phys. A*, 629, pp. 635-655.

[13] A. Boudard, J. Cugnon, J.-C. David, S. Leray, D. Mancusi (2013), "New potentialities of the Liège intranuclear cascade model for reactions induced by nucleons and light charged particles", *Phys. Rev. C*, 87, p. 014606.

[14] A. Kelić, M.V. Ricciardi, K.-H. Schmidt (2008), "ABLA07 – Towards a Complete Description of the Decay Channels of a Nuclear System from Spontaneous Fission to Multifragmentation", *IAEA INDC(NDS)-0530*, pp. 181–222.

[15] CINDER1.05, NEA-databank CCC-0755, https://rsicc.ornl.gov/, http://www.oecd-nea.org/tools/abstract/detail/CCC-0755/.

[16] F.X. Gallmeier et al. (2007), "An Environment using Nuclear Inventory Codes in Combination with the Radiation Transport Code MCNPX for Accelerator Activation Problem", *Proc. of the 8th Int. Topical Meeting on Nuclear Applications and Utilization of Accelerators*, Pocatello, US, p. 207.

[17] W.B. Wilson et al. (1995), "Recent Developments of the CINDER'90 Transmutation Code and Data Library for Actinide Transmutation Study", *Proc. GLOBAL'95 Int. Conf. on Evaluation of Emerging Nuclear Fuel Cycle Systems*, Versailles, France.

[18] R. Forrest (2007), "FISPACT-2007: User manual", *UKAEA FUS 534*, UKAEA.

[19] R. Forrest, J. Kopecky, and J.-C. Sublet (2007), "The European Activation File: EAF-2007 neutron-induced cross section library", *UKAEA FUS* 535, UKAEA.

[20] R. Keil (1999), "Chemical analysis of lead from SINQ target 4", *Analysis No. 7129*, PSI.

[21] R. Bimbot, H. Jaffrezic, Y. Le Beyec, M. Lefort, A. Vigny-Simon (1969), "Étude du mécanisme des réactions nucléaires induites par particules α de haute énergie I. Réactions 206Pb(α,xn)210-xPo", *J. de Physique,* 30[7], pp. 513–520.

[22] W. John (1956),"Excitation Functions for (α,xn) Reactions on Lead", *Phys. Rev.,* 103, pp. 704-713.

[23] G. Battistoni, S. Muraro, P.R. Sala, F. Cerutti, A. Ferrari,S. Roesler, A. Fasso, J. Ranft (2007), "The FLUKA code: Description and benchmarking", *AIP Conference Proceeding 896*, pp. 31-49.

[24] S. Agostinelli et al. (2003), "Geant4 - A Simulation Toolkit", *Nucl. Instr. & Meth. A*, 506, pp. 250-303.

[25] N.V. Mokhov (2010), "Recent Mars15 developments: nuclide inventory, DPA and gas production" ,*Fermilab-Conf-10-518-APC*.

[26] T. Ogawa, S. Hashimoto, T. Sato, K. Niita (2014), "Development of gamma de-excitation model for prediction of prompt gamma-rays and isomer production based on energy-dependent level structure treatment", *Nucl. Instr. Meth. B*, 325, pp. 35-42.

[27] A. Ferrari, private communication during the SATIF-12 workshop.